

Communication

A Novel Method for Fast Configuration of Energy Storage Capacity in Stand-Alone and Grid-Connected Wind Energy Systems

Haixiang Zang ^{*}, Mian Guo, Zeyu Qian, Zhinong Wei and Guoqiang Sun

College of Energy and Electrical Engineering, Hohai University, Nanjing 211100, China;
hhuguomian@163.com (M.G.); journaly_qianzeyu@126.com (Z.Q.); wzn_nj@263.net (Z.W.);
hhusunguoqiang@163.com (G.S.)

* Correspondence: zanghaixiang@hhu.edu.cn

Academic Editor: Andreas Sumper

Received: 1 July 2016; Accepted: 15 December 2016; Published: 17 December 2016

Abstract: In this paper, a novel method is proposed and applied to quickly calculate the capacity of energy storage for stand-alone and grid-connected wind energy systems, according to the discrete Fourier transform theory. Based on practical wind resource data and power data, which are derived from the American Wind Energy Technology Center and HOMER software separately, the energy storage capacity of a stand-alone wind energy system is investigated and calculated. Moreover, by applying the practical wind power data from a wind farm in Fujian Province, the energy storage capacity for a grid-connected wind system is discussed in this paper. This method can also be applied to determine the storage capacity of a stand-alone solar energy system with practical photovoltaic power data.

Keywords: discrete Fourier transform (DFT); energy storage; stand-alone system; wind power data

1. Introduction

In the past decades, renewable energy, represented by solar and wind generation, has gradually become essential in terms of energy structure [1–3]. Taking wind power as an example, its global cumulative installed capacity kept the acceleration rate around 13% in the past five years. However, a series of drawbacks, such as intermission randomness of renewable energy, must be considered with the promotion of new forms of generation [4,5]. Otherwise, stability and safety problems caused by renewable energy generation may become a serious problem in a modern power systems [6].

One approach to tackle these problems is to install energy storage facilities in wind farms or PV plants. By choosing an appropriate operation strategy, an energy storage system (ESS) could stabilize the fluctuation power generated into the grid by storing or releasing power [7]. Therefore, the appropriate capacity of an ESS plays an important goal in maintaining the stability and safety of the power grid [8,9]. Some studies mainly focused on minimizing the ESS size of solar or wind power forecasts from the perspective of operation performance and economic cost (Sreeraj et al. [9], Heide et al. [10], Chen et al. [11], Yang et al. [12], Celik et al. [13], Askari and Ameri [14,15], Fossati et al. [16], Ogunjuyigbe et al. [17], Berrada and Loudiyi [18] and many more).

Meanwhile, other researchers (Datta et al. [19], Ahmed et al. [20], Wang et al. [21], Abbassi and Chebbi [22], Makarov et al. [8], and Cao et al. [5]) calculated the configuration of ESSs based on time-domain or frequency-domain filtering methods to stabilize fluctuation in the regional tie-line. Generally, the ideal low-pass filtering method based on discrete Fourier transform (DFT) is recognized as an efficient way to filter power at a high frequency, which finally smooths the transmission power in the tie-line.

In this paper, a novel method based on DFT is developed to generate the capacity of an energy storage system for stand-alone and grid-connected wind energy systems. Wind power data used in this study are obtained from HOMER software (Homer Pro-3.7.6, HOMER Energy LLC, Colorado, CO, USA) and an actual wind farm, respectively. Furthermore, discussions relating to the configuration of ESSs for wind energy systems (both off-grid and grid-connected) are carried out.

The structure of this paper is organized as follows. Section 2 describes the data used for the analysis. Section 3 gives details about the proposed method. A discussion of the results is presented in Section 4, and Section 5 draws the conclusion.

2. Data Used

In this paper, wind energy systems (both off-grid and grid-connected) are investigated. For the stand-alone wind energy system, the practical wind speed data (at $39^{\circ}54' N, 105^{\circ}14' W$) exported from the American Wind Energy Technology Center are derived into HOMER software [23,24] to calculate the actual wind power according to the selected wind turbine type. HOMER is a micropower system optimization software, which can perform thousands of simulations to find the optimal configuration of both off-grid and grid-connected microgrid systems. The stand-alone wind energy system includes wind turbines as the energy generator, which is presented in the following sections, and they are established for gaining the wind power data. The rated power of the wind turbine type is 3.2 kW (12 machines for the optimization result). Figure 1 shows the wind power data of an isolated grid system all year and in January, respectively. The average value of the wind power is 5.9 kW, and its maximum value reaches 37.9 kW.

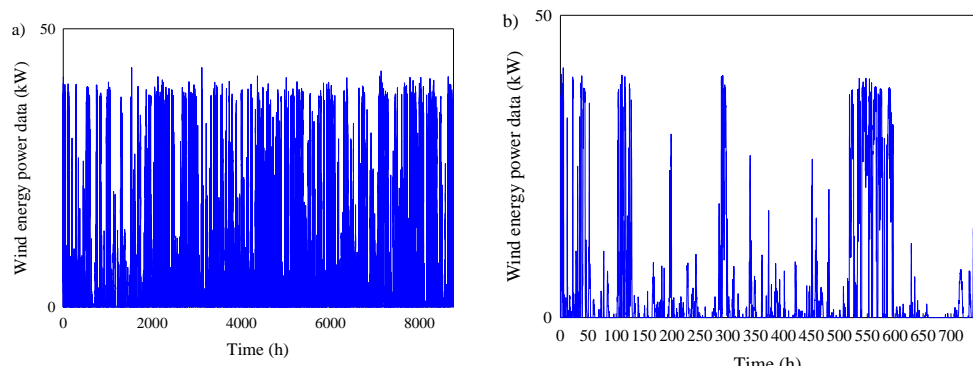


Figure 1. Wind power data for an isolated grid system (a) the whole year; (b) January.

For the grid-connected wind energy system, the practical wind power data is collected from an actual wind farm (Fujian Province in China). Figure 2 shows the wind power data of the grid-connected system all year and in January, respectively. The average value of the wind power is 33.0 MW.

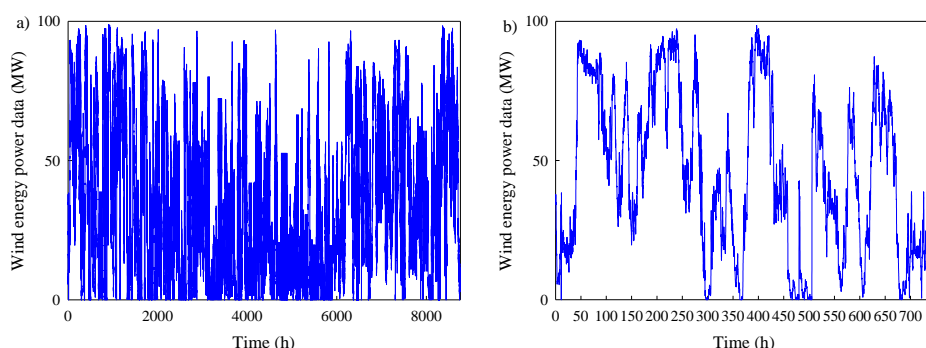


Figure 2. Wind power data for grid-connected wind system (a) the whole year; (b) January.

3. Methods Used

In this paper, a novel method for the fast configuration of the energy storage capacity is proposed based on the analysis of wind power. The procedure of calculating the capacity of the energy storage system consists of four steps, the description of which is given as follows:

Step 1: The amplitude-frequency curve of the wind power data is obtained through DFT. The following formula (Equation (1)) demonstrates the results calculated by DFT [25–27].

$$\begin{cases} \mathbf{S} = F(\mathbf{P}) = [S[1], \dots, S[i], \dots, S[N]]^T \\ f = [f[1], \dots, f[i], \dots, f[N]]^T \end{cases} \quad (1)$$

where N is the total number of sampling points; \mathbf{P} is the wind power data vector, $\mathbf{P} = [P[1], \dots, P[i], \dots, P[N]]^T$; $F(\mathbf{P})$ means the process of calculating the discrete Fourier transformation of the wind power data; $S[i]$ is the amplitude at the i th $f[i]$, $S[i] = R[i] + jI[i]$, with $R[i]$ and $I[i]$ representing the real part and the imaginary part, respectively; $f[i] = f(i-1)/N$, with f denoting the sampling frequency.

Step 2: To eliminate the DC component of the original power data, the amplitude for the zero frequency component is set to zero. The results can be obtained as follows (Equation (2)):

$$S_0[i] = \begin{cases} 0 + j0 & f_i = 0 \\ S[i] & f_i \neq 0 \end{cases} \quad (2)$$

The results of the wind power data without the DC component can be calculated (Equation (3)) by the inverse DFT.

$$\mathbf{P}_0 = F^{-1}(\mathbf{S}_0) = [P_0[1], \dots, P_0[i], \dots, P_0[N]]^T \quad (3)$$

where $F^{-1}(\mathbf{S}_0)$ means the inverse DFT; $P_0[i]$ is the wind power data at the i th sampling number without the DC component.

Step 3: Assuming a special frequency f ($T = 1/f$), a set of filtering wind power data can be acquired through Equations (4) and (5).

$$S_1[i] = \begin{cases} 0 + j0 & f_i < f \\ S_0[i] & f_i \geq f \end{cases} \quad (4)$$

$$\mathbf{P}_1 = F^{-1}(\mathbf{S}_1) = [P_1[1], \dots, P_1[i], \dots, P_1[N]]^T \quad (5)$$

where $F^{-1}(\mathbf{S}_1)$ means calculating the inverse DFT of \mathbf{S}_1 ; $P_1[i]$ is the filtering wind power data at the i th sampling number. Moreover, the period of the filtering wind power data, P_1 , ranges from 0 to T .

The energy of the signal which is the wind power data in this paper is defined as follows.

$$E = \sqrt{\sum_{i=1}^N x[i]^2} \quad (6)$$

where E is the energy of the signal; $x[i]$ is the signal data.

The energy of the wind power data P_0, P_1 , namely E_0 and E_1 , is calculated based on Equation (6). Also, the energy of the wind power data P_0 is chosen as the standard energy. The energy ratio can be computed by the following Equation (7).

$$\eta = E_1 / E_0 \quad (7)$$

The specific process of step 3 is as follows:

- (a) Set the energy ratio η_0 .

- (b) Calculate the different P_1 by changing the range of the pass band from low (f_{\min}) to high (f_{\max}) according to Equations (4) and (5) shown in the former step. Calculate the energy ratio between energy E_1 and the standard energy using Equations (6) and (7).
- (c) Determine the computing time T , which is the reception of the compensation frequency f . The program terminates and the final frequency f can be returned when the energy ratio η reaches the predefined value ($\eta - \eta_0 <= 0.005$).

Step 4: The method of determining the computing time is an important part of this paper. An optimal configuration method for energy storage is proposed in an ideal situation. Instead, the calculated power of the energy storage system is overlooked in this paper. The calculated power of the energy storage system is set as the average value of the original wind power P , while the capacity of the energy storage system can be obtained by calculating the product of the time and the calculated power.

4. Results and Discussion

By applying the above procedure, the capacity of the energy storage system for a stand-alone wind storage system and grid-connected wind system is calculated through the wind power data (Figures 1 and 2). The detailed procedure for the stand-alone wind energy system is as follows.

In step 1, based on the spectral analysis method, the amplitude-frequency characteristic curve of the wind power data for the stand-alone wind energy system (Figure 1) is obtained, as shown in Figure 3. In Figure 3, the amplitude of the wind power data is 5.9 when f equals 0, and the value is close to 0 when f is greater than 2×10^{-4} Hz. The magnitude of the signal amplitude in the spectrum characteristic curve, to a certain extent, reflects the strength of the signal at the corresponding frequency. It can be found that the energy of the wind power data concentrates at the frequency below 1×10^{-4} Hz.

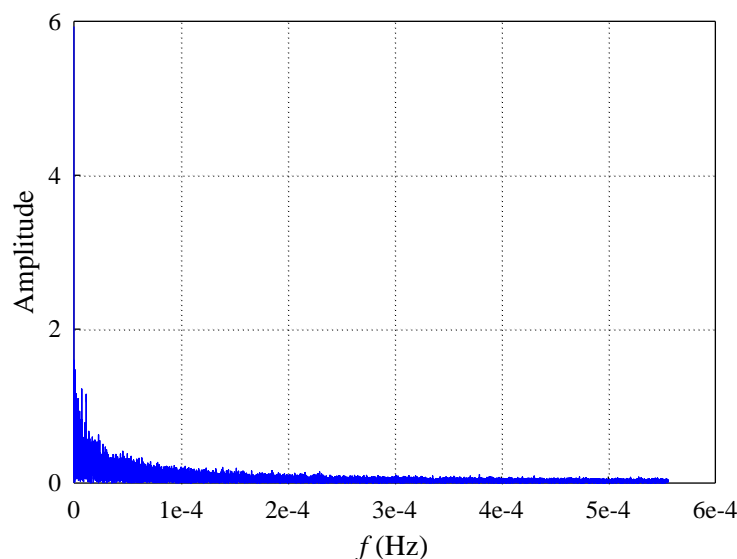


Figure 3. The amplitude-frequency characteristic curve of the wind power data.

In step 2, the amplitude for when the frequency equals zero (Figure 4) is set to zero using Equation (2). The new wind power data without the DC component (Figure 5) are obtained by the inverse DFT. It can be found that they are the same as the shape of the graph through a comparison between Figures 1 and 4. Moreover, the values of the wind power for Figure 4 are 5.9 kW lower than the wind power values of Figure 1, in general.

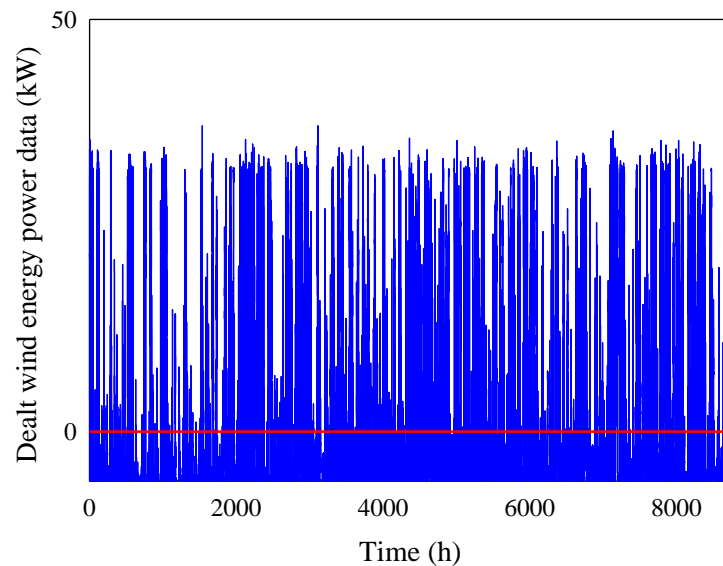


Figure 4. The original wind power data without the DC component.

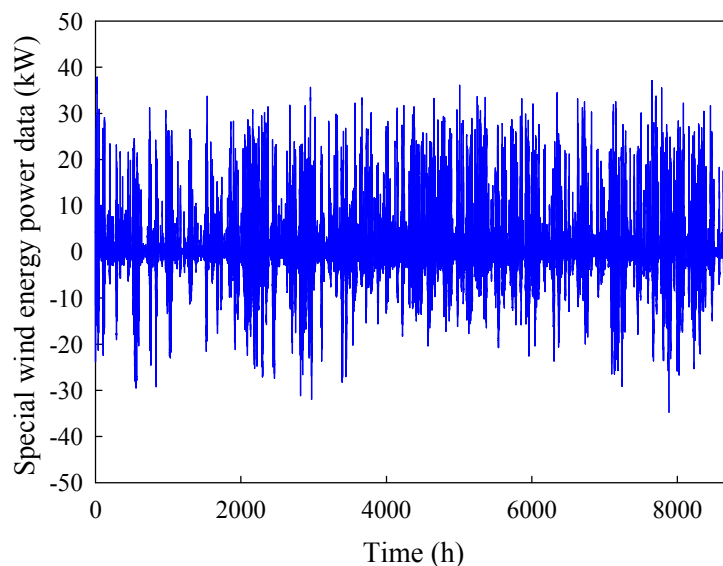


Figure 5. The superposed remaining signal, the energy of which accounts for 70% of the energy of the wind power data.

In the next step, the energy ratio η_0 is set to be 70% (taking 70% as an example) to study the energy storage configuration time. Based on Equations (4)–(7) and the specific process of the third step, the special frequency is calculated as 1.2684×10^{-5} Hz and the corresponding computing time is 21.9 h (Table 1). In the process of determining the computing time, the superposed remaining (70%) and filtering (30%) signal of the original wind power data are demonstrated in Figures 5 and 6, respectively.

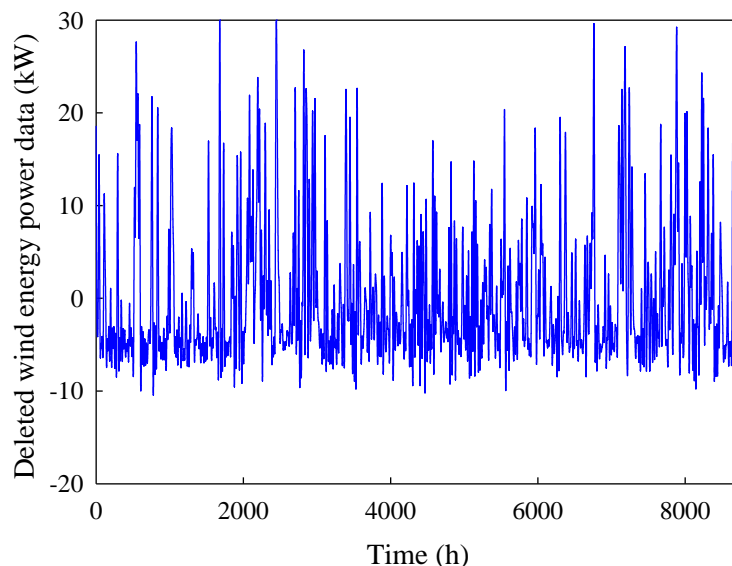


Figure 6. The superposed filtering signal, the energy of which accounts for 30% of the energy of the wind power data.

In the final step, the average value of the original wind power (5.9 kW) is chosen as the calculated power of a stand-alone wind energy system. The capacity of the energy storage system is obviously estimated by the calculated power and the corresponding time. Table 1 demonstrates the corresponding storage configuration results of the stand-alone wind energy system with different energy ratios η_0 . As shown in Table 1, in order to extract 90% energy of the wind generation power, the configuration time should be set as 130.7 h. However, the computing time is too long to retain higher economic benefits. In contrast, if the energy ratios are 80%, 70%, and 60%, the corresponding computing time can decrease to 45.1 h, 21.9 h and 10.9 h. Correspondingly, the energy storage capacity is 266 kWh, 129 kWh, and 64 kWh, respectively. In these three situations, the economy of the entire system is better. Moreover, if there is a wind power failure, the energy storage system can still meet the power supply of the important load.

Table 1. Configuration results of the energy storage system for the stand-alone wind energy system with different energy ratios.

Energy Ratio	Computing Time/h	Calculated Power/kW	Energy Storage Capacity/kWh
90%	130.7	5.9	771
80%	45.1	5.9	266
70%	21.9	5.9	129
60%	10.9	5.9	64
50%	6.0	5.9	35
40%	3.5	5.9	21

The stand-alone wind energy system is a combination of a wind turbine, battery bank, and inverter converting electricity between DC and AC as shown in Figure 7. The control unit of the wind turbine is a maximum power point tracker (MPPT) to extract the maximum possible energy, regardless of the variation in weather conditions. In the paper, an autonomous stand-alone wind energy system is used to meet the electricity requirements of a typical residential load (59.15 kWh per day with 5.63 kW peak power).

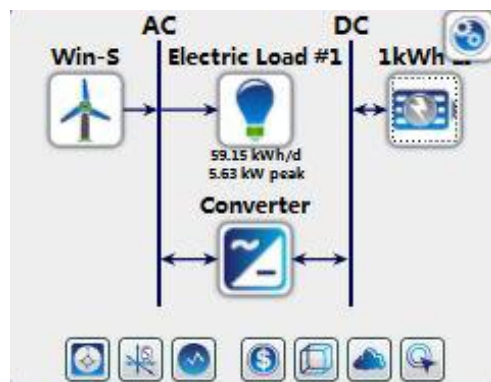


Figure 7. Stand-alone wind energy system.

HOMER simulates all the possible system configurations that meet the suggested load under the given conditions of wind resources. Moreover, the generated wind power data is used for the above research. This stand-alone system with 38.4 kW wind turbines (each wind turbine has a rated power of 3.2 kW), a 20 kW converter and 150 strings of batteries (each battery has a nominal capacity of 1 kWh) comprises an optimal power system. Compared with the proposed method, the value of 150 kWh for the energy storage capacity is between 127 kWh (energy ratio, 70%) and 266 kWh (energy ratio, 80%). Moreover, it is very close to the results when the energy ratio is 70%. The results show some effectiveness of the proposed approach.

Additionally, the proposed approach in the paper is also applied to configure the energy storage capacity for a grid-connected wind energy system. Based on the above process, the corresponding storage configuration results for a grid-connected wind system with different energy ratios η_0 are shown in Table 2. When the energy ratios are 25%, 20%, and 15%, the corresponding energy storage capacity is 396 MWh, 257.4 MWh, and 128.7 MWh, respectively. The energy storage capacity is chosen based on the tradeoff between the investment demand of a large capacity storage reserve and the output stability of the wind farm.

Table 2. Configuration results of the energy storage system for the grid-connected wind system with different energy ratios.

Energy Ratio	Computing Time/h	Calculated Power/MW	Energy Storage Capacity/MWh
40%	30.0	33.0	990.0
35%	23.8	33.0	785.4
30%	19.2	33.0	633.6
25%	12.0	33.0	396.0
20%	7.8	33.0	257.4
15%	3.9	33.0	128.7
10%	1.5	33.0	49.5

5. Conclusions

With technological improvements in the energy field, energy storage systems (ESSs) are exerting increasingly a profound influence on the future electrical grid. Based on the above step-by-step procedure for the proposed method, the capacity of the energy storage system for stand-alone and grid-connected wind energy systems is configured and analyzed. In this paper, the ESS capacity for a stand-alone wind energy system is produced and investigated using wind power data derived from the American Wind Energy Technology Center and HOMER software. Taking the energy ratio η_0 (70%) as an example, the energy storage computing time is analyzed in detail in this work. It is obvious that the configuration time (130.7 h) is too long to retain higher economic benefits. The configuration results for other energy ratios (80%, 70%, and 60%) having better economy are shown in the tabulation. Moreover,

the energy storage system can meet the power supply for some of the important load. The EES capacity results are compared with the configuration capacity using HOMER software. In addition, the configuration results for a grid-connected wind system are analyzed in this study. The configuration time (with better economic benefit) for the energy ratios (25%, 20% and 15%) is 12.0 h, 7.8 h and 3.9 h respectively. For different targets, the energy ratio and the corresponding configuration result can be chosen and carried out by the proposed method (based on DFT theory).

For future studies, it will be interesting to investigate the appropriate configuration of an energy storage system for a hybrid complementary system with wind power and other renewable energy.

Acknowledgments: The research is supported by National Natural Science Foundation of China (51507052), the China Postdoctoral Science Foundation (2015M571653), the 111 Project (B14022), and the Fundamental Research Funds for the Central Universities (2015B02714).

Author Contributions: Haixiang Zang is the principal investigator of this work. He performed the simulations and wrote the manuscript; Mian Guo and Zeyu Qian contributed to the data analysis work and language editing; Zhinong Wei and Guoqiang Sun designed the simulation solutions and checked the whole manuscript. All authors revised and approved the manuscript for the publication.

Conflicts of Interest: The authors declare no conflict of interest.

References

1. Xu, X.; Niu, D.; Qiu, J.; Wu, M.; Wang, P.; Qian, W.; Jin, X. Comprehensive evaluation of coordination development for regional power grid and renewable energy power supply based on improved matter element extension and TOPSIS method for sustainability. *Sustainability* **2016**, *8*, 143. [[CrossRef](#)]
2. Liu, L.Q.; Wang, Z.X.; Zhang, H.Q.; Xue, Y.C. Solar energy development in China-A review. *Renew. Sustain. Energy Rev.* **2010**, *14*, 301–311. [[CrossRef](#)]
3. Chauhan, A.; Saini, R.P. Techno-economic feasibility study on Integrated Renewable Energy System for an isolated community of India. *Renew. Sustain. Energy Rev.* **2016**, *59*, 388–405. [[CrossRef](#)]
4. Banos, R.; Manzano-Agugliaro, F.; Montoya, F.; Gil, C.; Alcayde, A.; Gómez, J. Optimization methods applied to renewable and sustainable energy: A review. *Renew. Sustain. Energy Rev.* **2011**, *15*, 1753–1766. [[CrossRef](#)]
5. Cao, M.; Xu, Q.; Zeng, P.; Xu, X.; Yuan, X. An energy storage system configuration method to stabilize power fluctuation in different operation periods. In Proceedings of the 2014 IEEE PES General Meeting Conference & Exposition, Washington, DC, USA, 27–31 July 2014; IEEE: New York, NY, USA, 2014; pp. 1–5.
6. Cao, M.; Xu, Q.; Bian, H.; Yuan, X.; Du, P. Research on configuration strategy for regional energy storage system based on three typical filtering methods. *IET Gener. Transm. Distrib.* **2016**, *10*, 2360–2366. [[CrossRef](#)]
7. Hadjipaschalidis, I.; Poullikkas, A.; Efthimiou, V. Overview of current and future energy storage technologies for electric power applications. *Renew. Sustain. Energy Rev.* **2009**, *13*, 1513–1522. [[CrossRef](#)]
8. Makarov, Y.V.; Du, P.; Kintner-Meyer, M.C.; Jin, C.; Illian, H.F. Sizing energy storage to accommodate high penetration of variable energy resources. *IEEE Trans. Sustain. Energy* **2012**, *3*, 34–40. [[CrossRef](#)]
9. Sreeraj, E.; Chatterjee, K.; Bandyopadhyay, S. Design of isolated renewable hybrid power systems. *Sol. Energy* **2010**, *84*, 1124–1136. [[CrossRef](#)]
10. Heide, D.; Greiner, M.; Von Bremen, L.; Hoffmann, C. Reduced storage and balancing needs in a fully renewable European power system with excess wind and solar power generation. *Renew. Energy* **2011**, *36*, 2515–2523. [[CrossRef](#)]
11. Chen, S.; Gooi, H.B.; Wang, M. Sizing of energy storage for microgrids. *IEEE Trans. Smart Grid* **2012**, *3*, 142–151. [[CrossRef](#)]
12. Yang, H.; Lu, L.; Zhou, W. A novel optimization sizing model for hybrid solar-wind power generation system. *Sol. Energy* **2007**, *81*, 76–84. [[CrossRef](#)]
13. Celik, A.N.; Munee, T.; Clarke, P. Optimal sizing and life cycle assessment of residential photovoltaic energy systems with battery storage. *Prog. Photovolt. Res. Appl.* **2008**, *16*, 69–85. [[CrossRef](#)]
14. Askari, I.B.; Ameri, M. Optimal sizing of photovoltaic—Battery power systems in a remote region in Kerman, Iran. *Proc. Inst. Mech. Eng. A J. Power Energy* **2009**, *223*, 563–570. [[CrossRef](#)]
15. Baniasad Askari, I.; Ameri, M. The Effect of Fuel Price on the Economic Analysis of Hybrid (Photovoltaic/Diesel/Battery) Systems in Iran. *Energy Sources B Econ. Plan. Policy* **2011**, *6*, 357–377. [[CrossRef](#)]

16. Fossati, J.P.; Galarza, A.; Martín-Villate, A.; Fontán, L. A method for optimal sizing energy storage systems for microgrids. *Renew. Energy* **2015**, *77*, 539–549. [[CrossRef](#)]
17. Ogunjuyigbe, A.; Ayodele, T.; Akinola, O. Optimal allocation and sizing of PV/Wind/Split-diesel/Battery hybrid energy system for minimizing life cycle cost, carbon emission and dump energy of remote residential building. *Appl. Energy* **2016**, *171*, 153–171. [[CrossRef](#)]
18. Berrada, A.; Loudiyi, K. Operation, sizing, and economic evaluation of storage for solar and wind power plants. *Renew. Sustain. Energy Rev.* **2016**, *59*, 1117–1129. [[CrossRef](#)]
19. Datta, M.; Senju, T.; Yona, A.; Funabashi, T. Photovoltaic output power fluctuations smoothing by selecting optimal capacity of battery for a photovoltaic-diesel hybrid system. *Electr. Power Compon. Syst.* **2011**, *39*, 621–644. [[CrossRef](#)]
20. Ahmed, N.A.; Miyatake, M.; Al-Othman, A. Power fluctuations suppression of stand-alone hybrid generation combining solar photovoltaic/wind turbine and fuel cell systems. *Energy Convers. Manag.* **2008**, *49*, 2711–2719. [[CrossRef](#)]
21. Chengshan, W.; Bo, Y.; Jun, X.; Li, G. Sizing of energy storage systems for output smoothing of renewable energy systems. *Proc. CSEE* **2012**, *32*, 1–8.
22. Abbassi, R.; Chebbi, S. Energy management strategy for a grid-connected wind-solar hybrid system with battery storage: Policy for optimizing conventional energy generation. *Int. Rev. Electr. Eng.* **2012**, *7*, 3979.
23. Vallati, A.; Grignaffini, S.; Romagna, M. A New Method to Energy Saving in a Micro Grid. *Sustainability* **2015**, *7*, 13904–13919. [[CrossRef](#)]
24. Park, E.; Kwon, S.J. Solutions for optimizing renewable power generation systems at Kyung-Hee University's Global Campus, South Korea. *Renew. Sustain. Energy Rev.* **2016**, *58*, 439–449. [[CrossRef](#)]
25. Weinstein, S.; Ebert, P. Data Transmission by Frequency-Division Multiplexing Using the Discrete Fourier Transform. *IEEE Trans. Commun. Technol.* **1971**, *19*, 628–634. [[CrossRef](#)]
26. Wolf, J. Redundancy, the Discrete Fourier Transform, and Impulse Noise Cancellation. *IEEE Trans. Commun.* **1983**, *31*, 458–461. [[CrossRef](#)]
27. Zhongde, W. Fast algorithms for the discrete W transform and for the discrete Fourier transform. *IEEE Trans. Acoust. Speech Signal Process.* **1984**, *32*, 803–816. [[CrossRef](#)]



© 2016 by the authors; licensee MDPI, Basel, Switzerland. This article is an open access article distributed under the terms and conditions of the Creative Commons Attribution (CC-BY) license (<http://creativecommons.org/licenses/by/4.0/>).